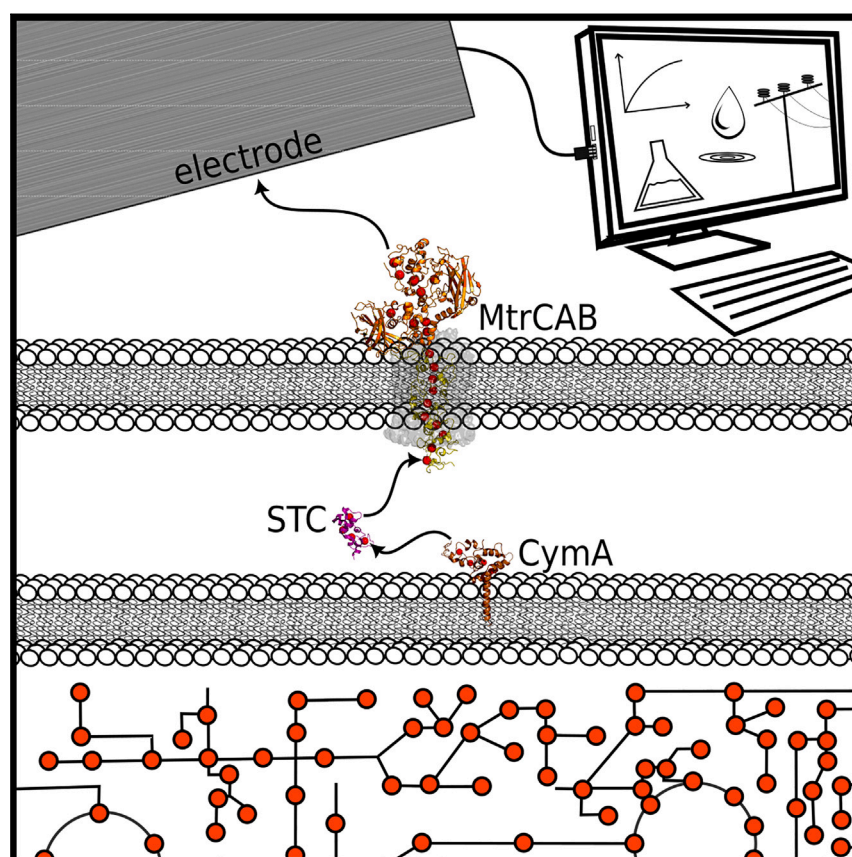


Article

Extracellular electron transfer pathways to enhance the electroactivity of modified *Escherichia coli*

Extracellular electron transfer (EET) is the ability of microbes known as exoelectrogens to reduce extracellular electron acceptors. This ability allows microbes to electronically link their metabolisms (depicted as the red network shown at the bottom) to electrodes for electrochemical applications in energy, synthesis, sensing, and bioremediation. We explored the expression of various cytochromes across the cellular envelope of *Escherichia coli* to improve EET. The highest electroactivity was achieved when the full metal-reducing pathway from *Shewanella oneidensis* MR-1, depicted as the MtrCAB, STC, and CymA in the figure, was expressed in *E. coli*. (PDB: 6R2Q, 6EE7)

Mohammed Mouhib, Melania Reggente, Lin Li, Nils Schuergers, Ardemis A. Boghossian

ardemis.boghossian@epfl.ch

Highlights

Expression of cytochromes enhances the electroactivity of *Escherichia coli*

Pathway composition determines electron transfer rates

Periplasmic electron shuttling is essential for high electroactivity

Thus engineered *E. coli* are a promising chassis for microbial electrochemical devices

Mouhib et al., Joule 7, 2092–2106
September 20, 2023 © 2023 The Authors.
Published by Elsevier Inc.
<https://doi.org/10.1016/j.joule.2023.08.006>



Article

Extracellular electron transfer pathways to enhance the electroactivity of modified *Escherichia coli*

Mohammed Mouhib,¹ Melania Reggente,¹ Lin Li,^{1,2} Nils Schuergers,^{1,3} and Ardemis A. Boghossian^{1,4,*}

SUMMARY

Escherichia coli (*E. coli*) show limited extracellular electron transfer (EET) that compromises their use in bioelectronics. We enhance the EET in *E. coli* by expressing an electron transfer pathway that spans the inner and outer membranes of the cell, including the periplasmic space in between. We observe a 54% enhancement in electron transfer for engineered *E. coli* expressing the endogenous inner-membrane NapC and periplasmic NapB cytochromes under non-native conditions with the outer-membrane MtrCAB complex from *Shewanella oneidensis* (*S. oneidensis*). The greatest enhancement, however, is observed for *E. coli* expressing the complete *S. oneidensis* Mtr pathway consisting of the inner-membrane CymA, periplasmic small tetraheme cytochrome (STC), and outer-membrane Mtr complex. This engineered strain shows a 3-fold increase in current generation compared with the empty vector control and a 2-fold increase compared with the state-of-the-art bioengineered strain comprising only the Mtr complex and CymA. These results highlight the importance of periplasmic shuttles in engineering EET.

INTRODUCTION

Bacteria are an inexhaustible natural resource and host to rich biochemical reaction networks. Their survival hinges on redox reactions for the interconversion of chemicals. These reactions have been exploited in a variety of industrial applications, both for synthesizing and consuming chemical substrates. Such substrates can be metabolized anabolically, requiring the net input of external energy,^{1,2} or catabolically, yielding a net generation of energy. Catabolic reactions are crucial to several green applications, including bioelectricity generation from organic substrates,³ reductive extracellular synthesis of valuable products such as nanoparticles^{4,5} and polymers,⁶ degradation of pollutants for bioremediation,⁷ and bioelectronic sensing.^{8,9} Many of these applications are facilitated by extracellular electron transfer (EET) mechanisms that electronically link the microbe's metabolism to an external electron acceptor, such as an electrode (Figure 1A).

Exoelectrogens are bacteria that have evolved inherent EET pathways.^{3,12} EET in these bacteria can occur through direct and/or indirect mechanisms.^{13–17} One of the best-characterized direct EET pathways is the metal-reducing (Mtr) pathway in *Shewanella oneidensis* (*S. oneidensis*) MR-1.¹⁷ In this pathway, electrons are transported across both insulating cellular membranes and the periplasmic space through a series of closely stacked hemes found in c-type cytochromes. The inner-membrane cytochrome CymA oxidizes quinol for electron transfer to various periplasmic cytochromes. These periplasmic cytochromes can subsequently transfer the extracted electrons extracellularly through the outer-membrane-spanning Mtr complex.¹⁷ Although exoelectrogens are effective for substrate and bioelectricity

CONTEXT & SCALE

Bioelectric bacteria are key to enabling living devices that rely on the transfer of electricity in and out of cells. These devices span energy applications including bioremediation, biological photovoltaics, microbial fuel cells, and electrosynthesis but are limited by poor extracellular electron transfer (EET) across the outer membrane. Although exoelectrogens, like *Shewanella oneidensis*, naturally express conduits that allow EET, their limited metabolisms and restricted genetic engineering tools hinder their use for most technologies. Microbes such as *Escherichia coli*, on the other hand, are renowned for their metabolic versatility, but they lack the EET abilities for bioelectronics.

We herein bioengineer *E. coli* that are capable of EET by introducing exogenous electron conduits, increasing electron transfer rates up to 3-fold. Beyond improving fuel cell performance, these bioengineered exoelectrogens pave the way for green applications currently hindered by EET.

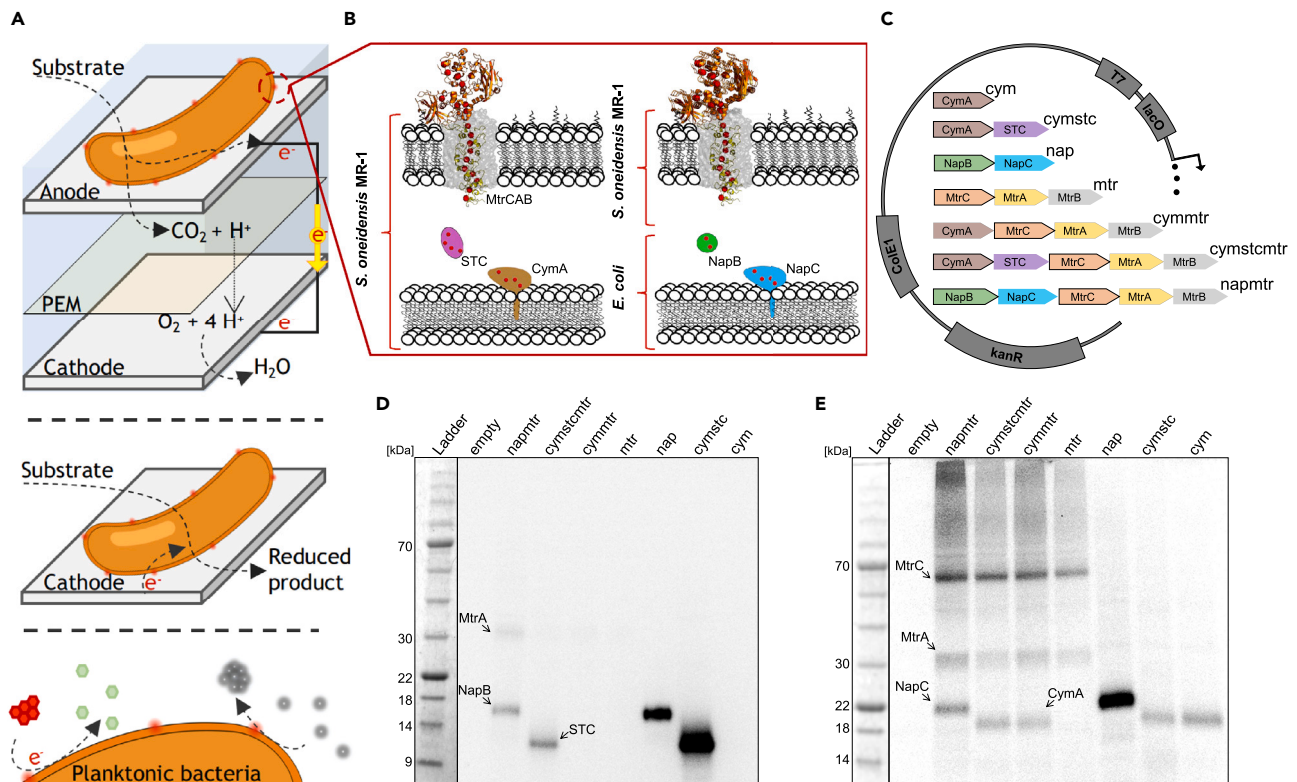


Figure 1. Expression of cytochrome pathways for improving EET

(A) Schematic of a microbial fuel cell (top), a biocathode for microbial electrosynthesis (middle), and electrode-free applications of EET for biosynthesis and bioremediation (bottom).

(B) Overview of the *S. oneidensis* MR-1 and *E. coli* cytochromes used in this study and their localization. The individual hemes are marked in red. (PDB: 6R2Q).

(C–E) (C) Constructs for the expression of engineered EET pathway variants and strain names. The *mtr* construct is based on the study by Jensen et al.,¹⁰ and the *cymmr* construct is based on the study by Jensen et al.¹¹ Size-separated cytochromes in the (D) periplasm and (E) membrane fractions of engineered strains. SDS-PAGE (D and E) was performed using 30 µg of protein per lane, 4%–20% polyacrylamide gels, and MOPS running buffer. Cytochromes were detected using enhanced chemiluminescence of the stained hemes.

interconversion, the exoelectrogens that are known to date lack the broad substrate spectrum and ease of metabolic engineering necessary for most microbial electrochemical applications.

Escherichia coli (*E. coli*), on the other hand, benefit from decades of metabolic research and readily available synthetic biology tools that can be exploited for a wide range of applications. Since *E. coli* are not considered natural exoelectrogens, they must be modified for EET. *E. coli* were previously engineered for EET through the heterologous expression of parts of the Mtr pathway.^{10,11,18–21} The electron transfer pathways differ among studies, ranging from the expression of single cytochromes^{19,20} to simultaneous expression of cytochromes in both cellular membranes¹¹ to co-expression of CymA in the inner membrane with periplasmic cytochromes.¹⁸ One of the most reconstituted strains to date has the Mtr complex expressed with CymA.¹¹ This electron conduit was recently co-expressed with ferredoxin and sulfide-quinone reductase modules to enable sulfide oxidation.²² The study showed that the charge generated from substrate oxidation by the modules could then be exported through the previously engineered electron conduit. The authors were therefore able to demonstrate the application of the co-expressed

¹Institute of Chemical Sciences and Engineering (ISIC), Ecole Polytechnique Fédérale de Lausanne (EPFL), 1015 Lausanne, Switzerland

²College of Environment and Ecology, Chongqing University, Chongqing 400045, China

³Molecular Genetics, Institute of Biology III, University of Freiburg, 79104 Freiburg, Germany

⁴Lead contact

*Correspondence: ardemis.boghossian@epfl.ch
<https://doi.org/10.1016/j.joule.2023.08.006>

MtrCAB and CymA conduit in a bioelectronic sensor for detecting thiosulfate in wastewater.

Despite these advances, the bioengineered EET efficiencies remain low, with questions remaining as to which cytochromes are essential for EET in engineered *E. coli*. For instance, the Mtr complex can be omitted in the presence of an extracellular redox mediator capable of diffusing into the periplasm.¹⁸ This omission reduces the metabolic cost of expressing the EET pathway, as the Mtr complex requires post-translational modification for the incorporation of 20 heme cofactors.^{13,23} However, such an omission may impede direct electron transfer and compromise the benefits of facilitated electron transfer between the redox mediator and additional membrane-bound proteins like MtrC. In fact, *E. coli* have even shown EET through the expression of membrane-bound cytochromes in the absence of periplasmic shuttles.¹¹ For example, previous studies have reported direct electron transfer from CymA to MtrA.²⁴ However, recent structural insights into the Mtr complex suggest that MtrA is anchored in the Mtr complex with the heme closest to the N terminus protruding only 2 nm into the periplasmic space.¹³ In addition, studies on electron transfer in *S. oneidensis* MR-1 highlight the importance of periplasmic cytochromes in EET.^{25,26} Given the similar widths of the periplasmic space in *E. coli* (~20–30 nm)^{27,28} and *S. oneidensis* MR-1 (~23.5 nm),²⁹ these findings suggest that co-expression of periplasmic cytochromes may enhance EET in engineered *E. coli* strains that express the Mtr complex. Although *E. coli* are not natively capable of respiration on extracellular solids, organic compounds can act as terminal electron acceptors in the periplasm under anaerobic conditions.³⁰ Overexpression of the associated cytochromes may thus improve EET in *E. coli*, especially in conjunction with heterologously expressed cytochromes that can facilitate electron transfer across the outer membrane.

Given the critical role of EET in microbial electrochemical devices, we aim here to construct an optimized EET pathway in *E. coli*. To this end, we express different EET pathways using components from both *S. oneidensis* MR-1 and *E. coli* distributed across the periplasmic space and the inner and outer membranes. We characterize the electron transfer using colorimetric assays based on the reduction of methyl orange and ferric citrate as soluble electron acceptors. The EET pathways with the highest electron transfer rates are then applied to a lactate-fueled microbial fuel cell.

RESULTS AND DISCUSSION

We developed two constructs based on the co-expression of the Mtr complex from *S. oneidensis* Mr-1 with a periplasmic and an inner-membrane protein (Figure 1B). The constructs allowed us to compare the performance of the Mtr complex in *E. coli* in combination with a *S. oneidensis*-derived and an *E. coli*-derived periplasmic pathway. Although the former is hypothesized to benefit from the native interaction between the periplasmic pathway and the Mtr complex, the latter is hypothesized to benefit from the native interaction between the periplasmic pathway and the microbe's cytosolic metabolism.

In the first construct (Figure 1B, left), we expressed the Mtr complex in the outer membrane along with the soluble cytochrome small tetraheme cytochrome (STC) in the periplasm and CymA in the inner membrane. Although *S. oneidensis* MR-1 harbors a large pool of cytochromes involved in electron transfer across the periplasm, STC was selected due to its role in electron transfer between CymA and

MtrA.^{25,31} In addition, the heterologous expression of STC alongside CymA and MtrA was previously shown to improve reduction of a soluble electron acceptor compared to other periplasmic cytochromes from *S. oneidensis* MR-1.¹⁸ Since electron transfer through CymA is believed to be limiting the electron transfer rates in engineered *E. coli*,³² its oxidation by STC is hypothesized to increase EET.

In the second construct (Figure 1B, right), we aerobically expressed the Mtr complex along with NapB in the periplasm and NapC in the inner membrane. Although both NapB and NapC are native to *E. coli*, they are only expressed under anaerobic conditions and further induced in the presence of nitrate,^{30,33} as these cytochromes are involved in the periplasmic reduction of nitrate. Although *E. coli* contains alternative periplasmic electron transfer pathways for different terminal electron acceptors, such as the Nrf and trimethylamine-N-oxide (TMAO) reductase systems for reducing nitrite and TMAO, respectively,³⁰ the nitrate reductase gene cluster presents several advantages. In particular, its inner-membrane protein NapC is similar to CymA in both sequence and function.²⁰ This similarity may favor electron transfer to the Mtr complex, which interacts natively with the CymA conduit in *S. oneidensis* MR-1. In addition, the NapB protein in *S. oneidensis* MR-1 may play a role in EET through the Mtr pathway.³⁴ In addition to the two complete pathways incorporating inner membrane, outer membrane, and periplasmic cytochromes, five partial pathways were expressed to evaluate the contributions of the different cytochromes to EET (Figure 1C). A summary of the constructs and their corresponding names is shown in Figure 1C.

SDS-PAGE was used to verify cytochrome expression and localization in the strains (Figures 1D, 1E, and S1). These samples were compared with a control strain with an empty vector backbone ("empty"). Compared with the control, the staining of the total protein content (Figure S1) showed indiscernible bands for nearly all the heterologous cytochromes, which appear to constitute a relatively low fraction of periplasmic and membrane proteins. Exceptionally, we observed a distinct protein band for STC in the total protein staining using a Coomassie dye, as its high expression levels allowed for detection together with other periplasmic proteins. The remaining proteins, however, were more readily discernible from the cytochrome staining. A comparison of the cytochrome staining of the periplasmic (Figure 1D) and membrane (Figure 1E) fractions shows that both STC and NapB were localized in the periplasm, as expected. However, much higher expression levels were observed in strains where the Mtr complex was omitted from the pathway. We hypothesize that the diminished expression in the presence of the Mtr complex may either be caused by decreased mRNA stability and secondary structures in longer transcripts that include the *mtrCAB* genes or competition of multiple co-expressed cytochromes for post-translational modification. Interestingly, MtrA was detected in both the periplasm and membrane fractions, whereas MtrC was only observed in the latter. The lack of a contaminating MtrC band in the periplasmic fractions indicates that the MtrA band in the periplasm does not stem from membrane fragments in the periplasmic fraction, an observation that agrees with previous reports.^{10,19} The cytochromes MtrC, MtrA, CymA, and NapC were all localized in the membrane fraction as expected.

To study the efficacies of the bioengineered pathways, we examined the ability of the different strains to reduce soluble electron acceptors (Figure 2A). We studied the reduction of two distinct acceptors, ferric citrate and methyl orange (C₁₄H₁₄N₃NaO₃S). The two acceptors were selected for their previous applications in monitoring microbial reduction. Ferric citrate and methyl orange show reduction

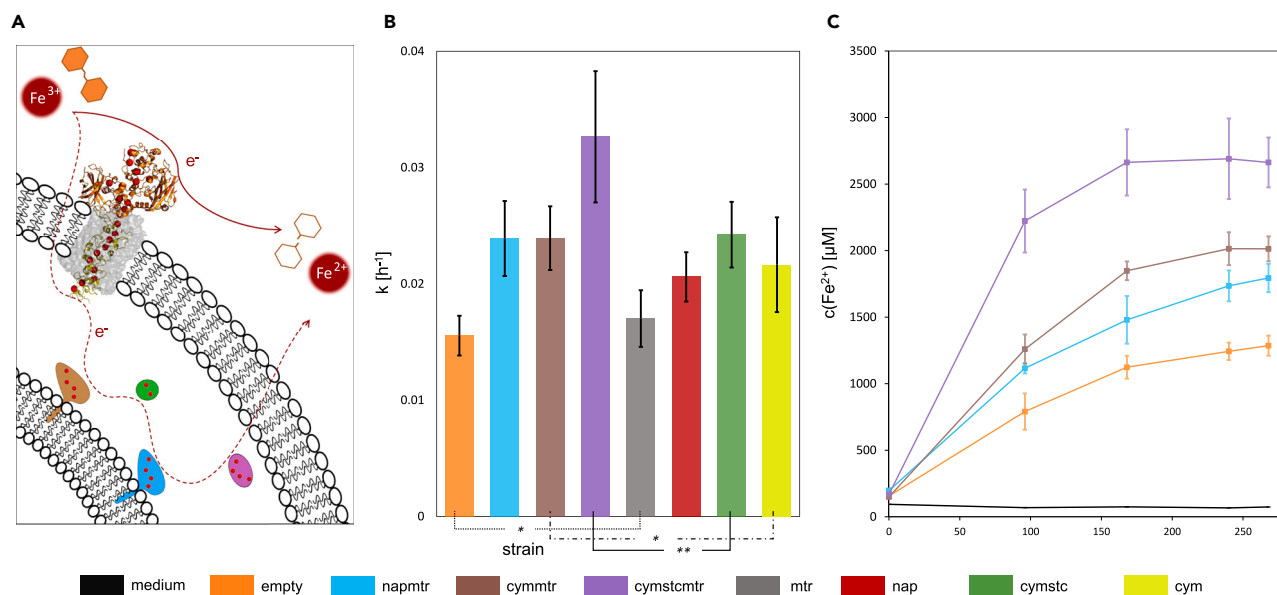


Figure 2. Electron transfer assays using soluble electron acceptors

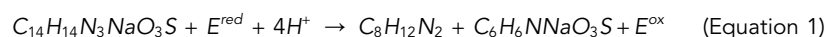
(A) Schematic illustration of methyl orange and ferric citrate reduction by engineered *E. coli*. (PDB: 6R2Q).

(B) Average reaction rate constants for the reduction of methyl orange by engineered *E. coli* compared with a control strain with an empty vector. Error bars represent 1 SD for 10–12 biological replicates. Plots of all individual replicates are shown in Figure S2, and the comparative analysis across the different strains is shown in Figure S3.

(C) Ferric citrate reduction over 11 days monitored using Fe²⁺ accumulation in assay media. Solid lines represent mean values, while error bars represent 1 SD for four biological replicates. Both reduction assays were carried out in minimal media with the respective electron acceptor under anaerobic conditions. *p < 0.15, **p < 0.01. p values were obtained from two tailed two sample t tests without assuming equal population variance (Welch's t test).

potentials in the range of –30 to +10 mV (vs. Ag/AgCl [3 M KCl], or equivalently, ca. +170 to +210 mV [vs. the standard hydrogen electrode (SHE)])³⁵ and 0 to +200 mV (vs. Ag/AgCl, or equivalently, ca. +200 to +400 mV [vs. SHE]),³⁶ respectively. These values lie largely above the reported ranges for the cytochromes in the outer-membrane electron acceptor of the microbe, MtrC (–450 to 0 mV [vs. SHE]³⁷; –325 to –25 mV [vs. SHE]³⁸; and –510 to +178 mV [vs. SHE]).³⁹ These reagents can therefore serve as effective electron acceptors for this microbial pathway, as demonstrated in previous studies.^{11,40} As ferric citrate is further reported to penetrate the outer membrane of the microbe, these acceptors can also provide a mechanism for monitoring reduction of the periplasmic proteins in the pathway in addition to the outer membrane MtrC.

The methyl orange undergoes a loss of absorbance at 420 nm on reduction of the azo group,⁴¹ allowing the electron transfer to be monitored colorimetrically (Equation 1). Although methyl orange reduction occurs predominantly extracellularly, interaction with intracellular components is possible through redox mediators and potentially limited uptake of the dye.⁴² Over 2 days, we observed a decrease in the methyl orange concentration following a pseudo-first-order decay reaction (Equation 2; Figure S2A),



$$[C_{14}H_{14}N_3NaO_3S]_t = [C_{14}H_{14}N_3NaO_3S]_0 \times e^{-OD_{600}kt} \quad (\text{Equation 2})$$

where E^{red} is the electron donor to the dye, E^{ox} is the corresponding oxidized species, [C₁₄H₁₄N₃NaO₃S]_t is the dye concentration at time t, [C₁₄H₁₄N₃NaO₃S]₀ is the

initial dye concentration, and k is the reaction rate constant. The calculated rate constants (Equation 2) for 10–12 biological replicates per strain are summarized in Figure 2B, and the statistical significance of the differences between the strains was evaluated using Welch's t test (Figure S3). Except for the *E. coli* strain expressing only the Mtr complex (mtr, $p = 0.11$), all bioengineered pathways were found to significantly increase methyl orange reduction (Figures 2B and S3) compared with the control strain. The lowest performing strain was therefore the strain that lacked both an inner-membrane and periplasmic component (mtr). These results indicate that the exclusive expression of the outer-membrane Mtr complex has a negligible effect on improving EET. Considering that the expression of the Mtr complex may arguably increase the permeability of native redox mediators, these results also support an EET mechanism based on charge transfer through the conduit rather than increased diffusion of other redox mediators through the outer membrane. This hypothesis agrees with previous findings that have shown a substantial increase in electron transfer of the Mtr complex in the presence of the inner-membrane cytochrome CymA¹⁸, which we also observe with the cymmtr strain at comparable MtrA and MtrC expression levels. In contrast to the lowest performing mtr strain, the bioengineered strains that lacked the outer-membrane complex (nap, cymstc, and cym) still showed a relative increase in EET compared with the control strain. Therefore, inner and periplasmic electron transfers appear to be limiting the initial performance of the control strain. Interestingly, we observed comparable performances for the *S. oneidensis*-derived pathway in the presence (cymstc) and absence (cym) of the periplasmic component, despite the significant STC expression in the cymstc strain. These results suggest that the outer-membrane transfer may become limiting when inner and periplasmic cytochromes are expressed without the Mtr complex.

In agreement with this hypothesis, we observed improved relative performances for the strains that expressed the outer-membrane Mtr complex in conjunction with both the inner-membrane and periplasmic components (napmtr and cymstcmtr). We observed these improvements over corresponding MtrCAB-lacking strains (nap, cymstc, and cym, respectively) that had even higher periplasmic (NapB and STC) and inner-membrane (NapC) expression levels (Figures 1D, 1E, and S1B). We note, however, a stark improvement in the performance of the *S. oneidensis*-derived pathway (cymstcmtr) over that of the *E. coli*-derived pathway (napmtr). The difference in performance is comparable with the difference in the performance of the *S. oneidensis*-derived pathway (cymstcmtr) with that of the same pathway lacking the periplasmic STC component (cymmtr). Given that the inner, outer, and periplasmic cytochrome expression levels of the *E. coli*-derived pathway are at least comparable (if not slightly higher) than the corresponding levels in the *S. oneidensis*-derived pathway, we hypothesize that the performance of the NapB di-heme may be limiting the periplasmic electron transfer in the *E. coli*-derived pathway compared with the STC tetraheme in the *S. oneidensis*-derived pathway. The crucial role of the periplasmic component and its interaction with membrane-bound cytochromes in the *S. oneidensis*-derived pathway was also verified by the compositional analysis shown in Table 1.

We further examined the periplasmic electron transfer in the *S. oneidensis*-derived pathway using ferric citrate as the electron acceptor (Figures 2C and S4). Compared with methyl orange, ferric citrate can readily diffuse into the periplasm⁴³, and its reduction can be monitored using a colorimetric assay based on the complexation of Fe^{2+} with ferrozine.⁴⁴ Similar to the methyl orange results, the ferric citrate results showed significant improvement in electron transfer for the *E. coli*-derived pathway (napmtr), the *S. oneidensis*-derived pathway (cymstcmtr), and the *S.*

Table 1. Electron transfer assays using soluble electron acceptors

	Reference strain	$\frac{k_{\text{ref+MtrCAB/STC}} - k_{\text{ref}}}{k_{\text{ref}}} \times 100\%$	CI _{95%}	p
MtrCAB+	empty	9.4%	± 10.2%	0.11
	cym	10.5%	± 12.8%	0.12
	cymstc	34.7%	± 16.0%	0.0005
STC+	cym	11.9%	± 13.8%	0.1
	cymmtr	36.4%	± 14.9%	0.0004

Relative contribution of Mtr complex or STC co-expression to total reduction rates in different strains. $k_{\text{ref+MtrCAB/STC}}$ and k_{ref} indicate rate constants for the methyl orange reduction by the given reference strains with and without the addition of MtrCAB or STC in the pathway (Figure 2B). CI_{95%} designates the 95% confidence interval for the percent increase of $k_{\text{ref+MtrCAB/STC}}$ over k_{ref} , with p values given for the same comparisons and obtained using Welch's t test.

oneidensis-derived pathway lacking the STC component (cymmtr) compared with the control. The ferric citrate reduction also followed the same trend as the methyl orange reduction, with the *S. oneidensis*-derived pathway showing a 99.1% (± 21%, $p < 0.001$) increase in Fe^{2+} accumulation over the *E. coli*-derived pathway after 4 days. Interestingly, the *S. oneidensis*-derived pathway showed a substantial increase (+76% ± 20% after 4 days, $p < 0.001$) in ferric citrate reduction compared to the corresponding pathway lacking the periplasmic STC component, despite the ability of the ferric citrate to penetrate the outer membrane and access inner-membrane proteins in the periplasmic space. These results confirm that STC plays an important role in oxidizing CymA and translocating electrons across the periplasm, thus enabling reduction of ferric citrate both at MtrC and in the periplasm. Nonetheless, the STC-lacking pathway still showed slightly higher electron transfer than the complete *E. coli*-derived pathway. These findings suggest that the *E. coli*-derived pathway is limited by electron transfer into the periplasm.

Finally, we demonstrated the performance of the *S. oneidensis*-derived pathway in a single-chamber, lactate-based microbial fuel cell. The setup consisted of a graphite-felt electrode as the electron acceptor, a platinum wire as the counter electrode, and an Ag/AgCl reference electrode. The system achieved steady state under an applied bias of +0.2 V after 3 days, with the *S. oneidensis*-derived pathway (cymstcmtr) showing an approximately 2- and 3-fold higher current compared to the pathway lacking the periplasmic STC component (cymmtr) and the control strain, respectively (Figure 3A). Following chronoamperometry, cyclic voltammetry was performed at a scan rate of 2 mV/s, revealing a single irreversible oxidation peak centered at around +75 mV (vs. Ag/AgCl) in all tested strains (Figure S5). Given the lack of a corresponding reduction peak, the results suggest that the compound being oxidized at the electrode functions as a redox mediator that is microbially reduced.⁴⁵ The highest oxidation current was recorded for the cymstcmtr strain, followed by the cymmtr strain and, finally, the empty vector control, as observed from the chronoamperometry measurements.

To examine the mechanism of the higher EET rates, we compared the relative viability, electrode colonization, and substrate utilization of the cymstcmtr *E. coli* with that of the control empty and cymmtr strains. The OD₆₀₀ of the electrolyte after the chronoamperometry measurements showed no significant differences in growth among the strains (Figure 3B). In addition, all strains showed comparable levels of colony-forming units (CFUs) on the working electrodes (Figure 3B). This lack of growth differences indicates that the strains were comparatively viable, and the EET enhancement from the cymstcmtr strain is unlikely due to increased growth

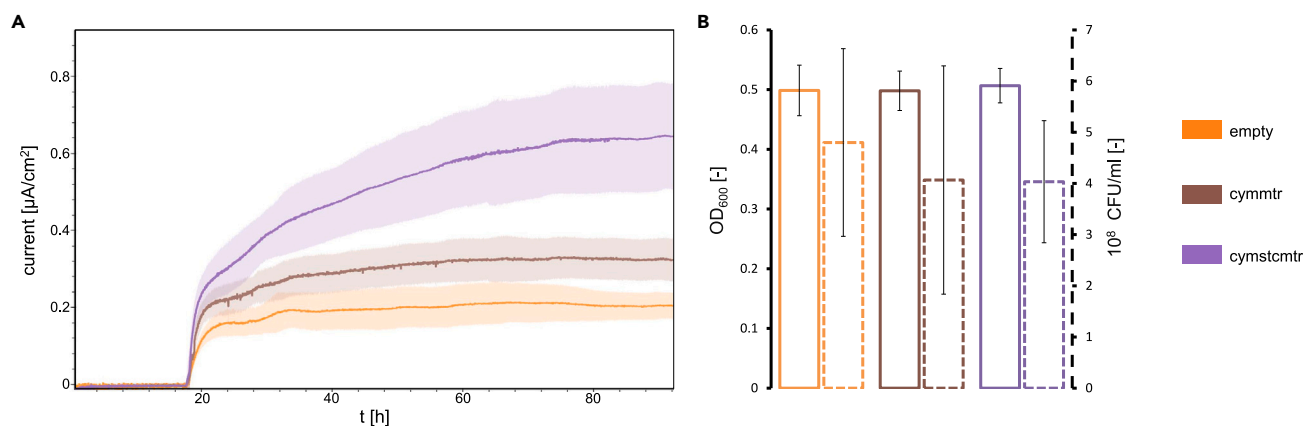


Figure 3. Electron transfer to graphite as the extracellular electron acceptor

(A) Chronoamperometry measurements in a lactate-fueled microbial cell. Measurements were taken under a positive applied bias of 0.2 V. Solid lines represent mean values, while shaded regions represent 1 SD for four biological replicates.

(B) Measurements of the OD₆₀₀ in the electrolyte (solid) and electrode colonization using CFU counts (dashed) from electrode extracts after chronoamperometry measurements. Mean values for four biological replicates are shown, with errors bars representing 1 SD.

or colonization of the electrode. We further compared the lactate consumption and formation of different fermentation products in the electrochemical cells using high-performance liquid chromatography (HPLC) (Figure S6). The HPLC measurements showed an overall decrease in lactate concentration and an increase in fermentation products, confirming the metabolization of the lactate over the course of the measurements. Furthermore, these measurements showed no significant differences among the strains, suggesting that the EET enhancements are unlikely to be due to increased catabolic conversion of the substrate. Together, these findings indicate that the increased current from the *S. oneidensis*-based pathway (cymstcmtr) likely stems from more efficient EET.

These observations suggest a promising basis for improving the performance of existing microbial technologies. The cymstcmtr pathway shows over a 2-fold enhancement in current production compared with the current state-of-the-art for bioengineered *E. coli* that is based on the cymmtr pathway.¹¹ Although this previous work showed that the cymmtr pathway was still over ~50 times slower than the native pathway in *S. oneidensis* MR-1, the bioengineered *E. coli* offer several advantages as microbial technologies. For example, *E. coli* can metabolize a broad range of substrates, and they can be readily engineered to consume an even larger range of unnatural substrates.^{46,47} As shown in Figure 4, *E. coli* can grow on brewery wastewater sourced from a local industrial plant. By contrast, the *S. oneidensis* MR-1 strain was unable to utilize this complex medium as a carbon source for growth. *E. coli* can also grow in minimal medium supplemented with highly abundant and industrially relevant feedstocks, such as glycerol as a byproduct of biodiesel production⁴⁸ and xylose as a main component of lignocellulosic biomass (Figure S7). *S. oneidensis* MR-1, by contrast, are unable to grow on these substrates, as reported in previous studies.^{49,50}

Conclusions

We examined the EET of bioengineered MtrCAB-based pathways in *E. coli* using methyl orange reduction. This assay was used to compare the EET of strains that couple the outer-membrane Mtr complex to either a *S. oneidensis*-derived (CymA-STC) or an *E. coli*-derived (NapC-NapB) inner-membrane/periplasmic

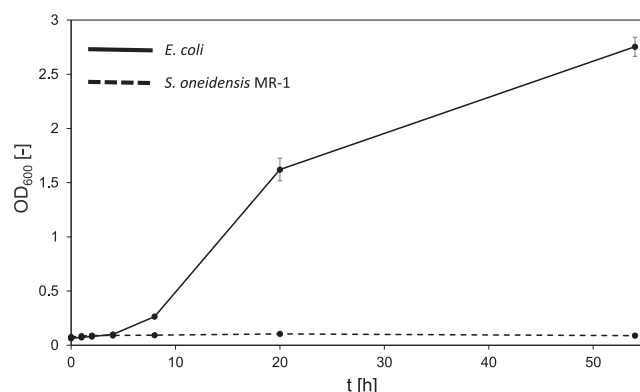


Figure 4. Brewery wastewater as a growth substrate for *E. coli* and *S. oneidensis* MR-1

Bacterial growth over time was determined using OD₆₀₀ measurements from aerobic culture flasks kept under constant shaking at 22°C. Lines represent mean values, while error bars represent 1 SD for three biological replicates.

pathway. Independent of the presence of the Mtr complex, we observed an increase for all strains expressing an inner-membrane (CymA or NapC) or periplasmic (STC or NapB) component. These results indicate periplasmic electron transfer to be rate-limiting in wild-type *E. coli*. The greatest relative electron transfer rates, however, were achieved for complete pathways comprising an inner-membrane, periplasmic, and outer-membrane components.

Of the two complete pathways that were studied, the strain harboring the *S. oneidensis*-derived pathway showed a significant improvement over that of the *E. coli*-derived pathway. The *E. coli*-derived pathway showed more limited electron transfer rates that were comparable with the *S. oneidensis*-derived strain that lacked its corresponding periplasmic component, STC. Similar trends were observed using the ferric citrate assay to monitor periplasmic reduction. Possibilities for improvement include the introduction of alternative periplasmic components and the optimization of their non-native interactions through techniques such as directed evolution.

The importance of these interactions is demonstrated through the enhanced performance of the *S. oneidensis*-derived pathway (cymstcmtr). This strain fully reconstitutes the Mtr pathway in *E. coli*, containing a total of 4 heterologously expressed cytochromes with 28 heme cofactors distributed across the periplasm and both cellular membranes. Importantly, we observed a 2-fold improvement in electron transfer compared with the state-of-the-art strain based on MtrCAB and CymA co-expression (cymmtr) in the absence of heterologously expressed periplasmic shuttles.^{11,22} Previous studies on the Mtr pathway in *S. oneidensis* MR-1^{25,26} similarly confirmed the importance of periplasmic electron transfer on overall EET. The improved extracellular and periplasmic reduction rates, along with the increased current production, in the presence of STC align with previous findings that have shown electron transfer across CymA to be limiting EET.³² The introduction of STC promotes the turnover of CymA to overcome the bottleneck electron transfer from CymA to MtrA. Future bioengineering approaches to enhance EET could therefore focus on the accumulation of NADH and quinols to increase electron transfer to the inner-membrane cytochrome. Furthermore, since the modification of the cytochrome c maturation (Ccm) machinery was previously shown to increase CymA expression levels,³² this strategy could be coupled with the STC-based

construct developed herein to further enhance the electroactivity of engineered *E. coli*.

The enhanced EET of the *cymstcmtr* strain thus brings a significant advantage to bioremediation and energy applications. The genetic amenability of *E. coli* allows this strain to be adapted to specific applications and feedstocks. This amenability translates into improved device performance and control. For example, it unlocks an industrial microbial fuel cell (MFC) technology that is less reliant on sub-optimal microbial consortia. Engineered consortia initially containing exoelectrogenic *E. coli*, such as the *cymstcmtr* strain herein, can be tailored to the feedstock through selective pressure. This approach, which has been conventionally limited to wild-type consortia, optimizes substrate conversion to electricity for a given feedstock. Such optimization is especially beneficial to industrial plants with effluents that are rich in organic waste, such as the brewery effluent used in this work, with the potential to offset operating costs. Besides MFCs, EET is also central to other applications such as electrosynthesis and biosensing. Improvements in EET thus promote higher synthesis yields as well as improved sensor kinetics in these respective industries. Beyond improving existing devices, these microbes inspire applications that are otherwise intractable without EET. These advancements therefore open the doors to new technologies in large-scale electrosynthesis or even electricity-based metabolic control.

EXPERIMENTAL PROCEDURES

Resource availability

Lead contact

Further information and requests for resources should be directed to and will be fulfilled by the lead contact, Ardemis A. Boghossian (ardemis.boghossian@epfl.ch).

Materials availability

Plasmids generated during this study are available upon request.

Data and code availability

All data are presented in the paper or [supplemental information](#), and no standardized datasets were generated during this study.

Plasmid preparation

All strains, plasmids, and primers can be found in [Table S1](#). *E. coli* DH5 α was used for all molecular cloning experiments. Plasmids pMO1 (*napBC*) and pMO₂ (*cymA*, *cctA*) were procured from GenScript using the pSB1ET2 plasmid as the backbone, with the sequence for *NapBC* from *E. coli* K12 MG1655 (genebank: CP032679.1) and the sequence for *CymA* and *STC* from *S. oneidensis* MR-1 (genebank: AE014299.2). The *mtrCAB* gene was amplified from plasmid I5049 using primers 1, 2 or 3, 4 for Gibson assembly⁵¹ with pMO1 (primers 5 and 6) and pMO₂ (primers 7 and 8), respectively, yielding plasmids pMO1.1 and pMO2.1. For the construction of pMO2.2, I5049 was cut (EcoRI and XbaI) for excision of the *mtrCAB* sequence, blunt-ended, and re-ligated. All genes were expressed in single operons under the control of an isopropyl β -D-1-thiogalactopyranoside (IPTG)-inducible promoter ([Figure 1C](#); [Table S1](#)). All constructs were co-expressed with the Ccm pathway using the pEC86 plasmid.⁵² This pathway, which is necessary for the post-translational incorporation of hemes, was expressed constitutively using a tet promoter on a separate plasmid. Although the *E. coli* genome contains native genes for the Ccm machinery, these genes are not expressed under aerobic conditions.

Bacterial growth

E. coli C43(DE3) were transformed with pEC86 and either pSB1ET2, pMO1, pMO1.1, I5023, pMO₂, pMO2.1, pMO2.2, or I5049 using electroporation and plated on 2xYT-agar plates with 50 µg/mL kanamycin (kan) and 34 µg/mL chloramphenicol (cam). Colonies were used to inoculate 5 mL 2xYT (kan, cam) medium and grown overnight (220 rpm, 37°C). Expression cultures (2xYT, kan, cam, 1 mM 5-aminolevulinic acid) were inoculated to an OD₆₀₀ of 0.1 and grown until an OD₆₀₀ of ~0.6 (220 rpm, 37°C). Cytochrome expression was then induced using 10 µM IPTG, and cultures were grown overnight (220 rpm, 30°C, 16 h).

To assess the growth of *E. coli* C43(DE3) and *S. oneidensis* MR-1 (Figures 4 and S7) in various media, overnight cultures were prepared free of antibiotics in 5 mL 2xYT medium using single colonies, and incubated at 37°C and 30°C, respectively (220 rpm shaking). Overnight cultures were washed twice (3,000 g, 4°C, 10 min) in either wastewater or M9-media with carbon sources as indicated (50 mM DL-lactate, 50 mM D-xylose, or 50 mM glycerol), and used to inoculate the respective growth media to an OD₆₀₀ of 0.1 (0.07 in wastewater). The growth was monitored using OD₆₀₀ measurements (UV-3600 Plus, Shimadzu) throughout incubation at indicated temperatures, under constant shaking (220 rpm). Brewery wastewater was sourced at a local industrial plant, autoclaved, and filtered through a 0.2 µm membrane prior to use.

Subcellular fractionation

Subcellular fractionation was adapted from Malherbe et al.⁵³ In brief, cytochrome expression cultures were harvested (3,000 g, 4°C, 15 min) to an OD₆₀₀ of 8 in 16 mL. Cells were washed in PBS (3,000 g, 4°C, 15 min), resuspended in buffer A (100 mM Tris-HCl pH 8, 500 mM sucrose, 0.5 mM EDTA), incubated for 5 min on ice, and centrifuged (3,000 g, 4°C, 15 min). For recovery of periplasmic proteins, the pellets were resuspended in 1 mM MgCl₂ and incubated for 2 min. After centrifugation (3,000 g, 4°C, 15 min), supernatants containing periplasmic proteins were concentrated using 3 kDa molecular weight cutoff Amicon filters.

For recovery of membrane proteins, the pellets were washed once in buffer B (50 mM Tris-HCl pH 8, 250 mM sucrose, 10 mM MgSO₄), resuspended in buffer C (50 mM Tris-HCl pH 8, 2.5 mM EDTA), and lysed via sonication. Lysates were collected following centrifugation (10,000 g, 10 min, 4°C), and membrane proteins were recovered by centrifugation (21,000 g, 4 h, 4°C) and washing in buffer C. The final pellet was resuspended in buffer C with 1% Triton X-100 at 4°C.

In-gel cytochrome staining

Proteins were separated according to size using SDS-PAGE (SurePage 4%–20% gels, GenScript; 1× NuPAGE lithium dodecyl sulfate sample buffer, Invitrogen; 3-(N-morpholino)propanesulfonic acid running buffer). Polyacrylamide gels were rinsed in distilled water, and excess water was removed before application of an enhanced chemiluminescence (ECL) stain (SuperSignal West Pico PLUS, Thermo Scientific) to the gel followed by incubation for 5 min. Gels were imaged for cytochromes using an ECL imaging system (Fusion solo S, Vilber).

Methyl orange

E. coli were harvested (3,000 g, 4°C, 15 min), washed in M9-glycerol medium,¹⁸ and resuspended in 10 mL M9 glycerol medium with 200 µM methyl orange to an OD₆₀₀ of 4. Cultures were sealed for anaerobic growth and stirred at room temperature for 3 days. Culture samples were taken with a syringe at set time intervals, and the OD₆₀₀

was monitored using a spectrophotometer (UV-3600 Plus, Shimadzu). After centrifugation of samples (22°C, 21,000 g, 3 min), clear supernatants were used for absorbance measurements at 465 nm in 96 well plates (Varioscan LUX, Thermo Scientific). Methyl orange was used as the sole electron acceptor under anaerobic conditions, with glycerol as the electron donor in minimal growth medium (M9). Experiments were carried out using 12 biological replicates per strain, and the resulting rate constants were normalized to an OD₆₀₀ of 1. All datasets were checked for outliers using the Grubbs' test. Differences in the mean methyl orange reduction rates were compared using two-tailed t tests, and the resulting probabilities are summarized in [Figure S3](#).

Ferric citrate reduction assay

E. coli were harvested (3,000 g, 4°C, 15 min), washed in M9 lactate medium,¹⁰ and resuspended in 10 mL M9 lactate medium with 10 mM Fe(III)-citrate to an OD₆₀₀ of 2. Cultures were sealed for anaerobic growth and stirred at room temperature for 11 days. Culture samples were taken with a syringe at set time intervals, and the OD₆₀₀ was monitored using a spectrophotometer (UV-3600 Plus, Shimadzu). For the Fe²⁺ measurements, samples were filtered (0.2 μM) and diluted to 50% in 1 M HCl. Absorbance was measured at 562 nm in 96-well plates immediately after the addition of 180 μL of a 1 g/L ferrozine solution to 20 μL of dilute samples. Measurements were taken for the complete EET pathways (cymstcmtr, napmtr), the Mtr pathway lacking periplasmic shuttling (cymmtr), and the empty vector control using three biological replicates.

Electrochemical setup and measurements

Electrochemical measurements were carried out in a single-chambered cell (100 mL bottle) with M9-lactate medium⁵⁴ as the electrolyte, a Pt wire counter electrode, an Ag/AgCl (3 M KCl) reference electrode and a 1 × 1.1 × 0.5 cm graphite-felt (Alfa Aesar) electrode connected to a Pt wire as the anode. Anodes were pretreated in piranha solution (97% H₂SO₄:30% H₂O₂ in 3:1 mixture) for 10 min, before washing and storage in distilled water. Experiments were run using a multichannel potentiostat (MultiPalmSens 4).

Bacteria (25 mL cultures, see [bacterial growth](#) section) were harvested (3,000 g, 4°C, 20 min) and washed 3 times in 10 mL of M9 medium with carbon sources as indicated. The washed pellets were resuspended in 5 mL of the same medium and used to inoculate electrolytes for a final volume of 100 mL. Electrolytes were supplemented with 50 μg/mL of kan and with IPTG to a final concentration of 10 μM. The chronoamperometry measurements were taken under constant stirring (10 mm long magnetic stirrer, lowest setting on a ThermoScientific Variomag Mono magnet) and flow of N₂(g) for anaerobic conditions. Cyclic voltammetry was performed using a scan rate of 2 mV/s in a potential range of −0.1 to 0.45 V, starting at a potential of 0 V against the Ag/AgCl reference electrode. After these measurements, the anodes were rinsed three times and incubated in PBS (2 h, 4°C, 15 mL) for characterization of bacterial growth using CFU counts.

HPLC analysis

Samples from electrochemical cells were filtered (0.2 μM) and separated on a Hi-plex H column (Agilent) using 14 mM H₂SO₄ as the mobile phase. The column temperature was kept constant at 40°C. Experiments were carried out on an Infinity II (Agilent) HPLC system, and compounds were detected using absorbance (210 nm) and refractive index measurements (Agilent 1260 DAD WR, 1260 RID).

SUPPLEMENTAL INFORMATION

Supplemental information can be found online at <https://doi.org/10.1016/j.joule.2023.08.006>.

ACKNOWLEDGMENTS

The authors are grateful for funding by the Gebert R f Stiftung, the Swiss National Science Foundation Assistant Professor (AP) Energy Grant (project no. PYAPP2_154269), and Swiss National Science Foundation project no. IZLIZ2_182972. The authors thank Prof. Caroline-Ajo Franklin for providing plasmids (pSB1ET2, I5049, and I5023) for cytochrome expression. The authors also thank Les Brasseurs brewery in Lausanne, Switzerland, for providing the wastewater sample for microbial growth measurements.

AUTHOR CONTRIBUTIONS

The project was conceptualized by M.M. and A.A.B. Experiments were performed by M.M., M.R., and L.L. All authors contributed to the data analysis and the writing and reviewing of this manuscript.

DECLARATION OF INTERESTS

The authors declare no competing interests.

Received: July 19, 2023

Revised: August 3, 2023

Accepted: August 17, 2023

Published: September 8, 2023

REFERENCES

- Jourdin, L., and Burdyny, T. (2021). Microbial electrosynthesis: where do we go from here? *Trends Biotechnol.* 39, 359–369. <https://doi.org/10.1016/j.tibtech.2020.10.014>.
- Tefft, N.M., and TerAvest, M.A. (2019). Reversing an extracellular electron transfer pathway for electrode-driven acetoin reduction. *ACS Synth. Biol.* 8, 1590–1600. <https://doi.org/10.1021/acssynbio.8b00498>.
- Logan, B.E. (2009). Exoelectrogenic bacteria that power microbial fuel cells. *Nat. Rev. Microbiol.* 7, 375–381. <https://doi.org/10.1038/nrmicro2113>.
- Tian, L.J., Li, W.W., Zhu, T.T., Chen, J.J., Wang, W.K., An, P.F., Zhang, L., Dong, J.C., Guan, Y., Liu, D.F., et al. (2017). Directed biofabrication of nanoparticles through regulating extracellular electron transfer. *J. Am. Chem. Soc.* 139, 12149–12152. <https://doi.org/10.1021/jacs.7b07460>.
- Dundas, C.M., Graham, A.J., Romanovicz, D.K., and Keitz, B.K. (2018). Extracellular electron transfer by *Shewanella oneidensis* controls palladium nanoparticle phenotype. *ACS Synth. Biol.* 7, 2726–2736. <https://doi.org/10.1021/acssynbio.8b00218>.
- Fan, G., Dundas, C.M., Graham, A.J., Lynd, N.A., and Keitz, B.K. (2018). *Shewanella oneidensis* as a living electrode for controlled radical polymerization. *Proc. Natl. Acad. Sci. USA* 115, 4559–4564. <https://doi.org/10.1073/pnas.1800869115>.
- Springthorpe, S.K., Dundas, C.M., and Keitz, B.K. (2019). Microbial reduction of metal-organic frameworks enables synergistic chromium removal. *Nat. Commun.* 10, 5212. <https://doi.org/10.1038/s41467-019-13219-w>.
- Webster, D.P., TerAvest, M.A., Doud, D.F.R., Chakravorty, A., Holmes, E.C., Radens, C.M., Sureka, S., Gralnick, J.A., and Angenent, L.T. (2014). An arsenic-specific biosensor with genetically engineered *Shewanella oneidensis* in a bioelectrochemical system. *Biosens. Bioelectron.* 62, 320–324. <https://doi.org/10.1016/j.bios.2014.07.003>.
- Yang, Y., Yu, Y.Y., Wang, Y.Z., Zhang, C.L., Wang, J.X., Fang, Z., Lv, H., Zhong, J.J., and Yong, Y.C. (2017). Amplification of electrochemical signal by a whole-cell redox reactivation module for ultrasensitive detection of pyocyanin. *Biosens. Bioelectron.* 98, 338–344. <https://doi.org/10.1016/j.bios.2017.07.008>.
- Jensen, H.M., Albers, A.E., Malley, K.R., Londer, Y.Y., Cohen, B.E., Helms, B.A., Weigle, P., Groves, J.T., and Ajo-Franklin, C.M. (2010). Engineering of a synthetic electron conduit in living cells. *Proc. Natl. Acad. Sci. USA* 107, 19213–19218. <https://doi.org/10.1073/pnas.1009645107>.
- Jensen, H.M., TerAvest, M.A., Kokish, M.G., and Ajo-Franklin, C.M. (2016). CymA and exogenous flavins improve extracellular electron transfer and couple it to cell growth in Mtr-expressing *Escherichia coli*. *ACS Synth. Biol.* 5, 679–688. <https://doi.org/10.1021/acssynbio.5b00279>.
- Koch, C., and Harnisch, F. (2016). Is there a specific ecological niche for electroactive microorganisms? *ChemElectroChem* 3, 1282–1295. <https://doi.org/10.1002/celec.201600079>.
- Edwards, M.J., White, G.F., Butt, J.N., Richardson, D.J., and Clarke, T.A. (2020). The crystal structure of a biological insulated transmembrane molecular wire. *Cell* 181, 665–673.e10. <https://doi.org/10.1016/j.cell.2020.03.032>.
- Wang, F., Gu, Y., O'Brien, J.P., Yi, S.M., Yalcin, S.E., Srikanth, V., Shen, C., Vu, D., Ing, N.L., Hochbaum, A.I., et al. (2019). Structure of microbial nanowires reveals stacked hemes that transport electrons over micrometers. *Cell* 177, 361–369.e10. <https://doi.org/10.1016/j.cell.2019.03.029>.
- Light, S.H., Su, L., Rivera-Lugo, R., Cornejo, J.A., Louie, A., Iavarone, A.T., Ajo-Franklin, C.M., and Portnoy, D.A. (2018). A flavin-based extracellular electron transfer mechanism in diverse Gram-positive bacteria. *Nature* 562, 140–144. <https://doi.org/10.1038/s41586-018-0498-z>.
- Mouhib, M., Antonucci, A., Reggente, M., Amirjani, A., Gillen, A.J., and Boghossian, A.A. (2019). Enhancing bioelectricity generation in microbial fuel cells and biophotovoltaics using nanomaterials. *Nano Res.* 12, 2184–2199. <https://doi.org/10.1007/s12274-019-2438-0>.

17. Shi, L., Dong, H., Reguera, G., Beyenal, H., Lu, A., Liu, J., Yu, H.Q., and Fredrickson, J.K. (2016). Extracellular electron transfer mechanisms between microorganisms and minerals. *Nat. Rev. Microbiol.* 14, 651–662. <https://doi.org/10.1038/nrmicro.2016.93>.
18. Sturm-Richter, K., Golitsch, F., Sturm, G., Kipf, E., Dittich, A., Beblawy, S., Kerzenmacher, S., and Gescher, J. (2015). Unbalanced fermentation of glycerol in *Escherichia coli* via heterologous production of an electron transport chain and electrode interaction in microbial electrochemical cells. *Bioresour. Technol.* 186, 89–96. <https://doi.org/10.1016/j.biortech.2015.02.116>.
19. Pitts, K.E., Dobbin, P.S., Reyes-Ramirez, F., Thomson, A.J., Richardson, D.J., and Seward, H.E. (2003). Characterization of the *Shewanella oneidensis* MR-1 decaheme cytochrome MtrA: expression in *Escherichia coli* confers the ability to reduce soluble Fe(III) chelates. *J. Biol. Chem.* 278, 27758–27765. <https://doi.org/10.1074/jbc.M302582200>.
20. Gescher, J.S., Cordova, C.D., and Spormann, A.M. (2008). Dissimilatory iron reduction in *Escherichia coli*: identification of CymA of *Shewanella oneidensis* and NapC of *E. coli* as ferric reductases. *Mol. Microbiol.* 68, 706–719. <https://doi.org/10.1111/j.1365-2958.2008.06183.x>.
21. Wu, Z., Wang, J., Liu, J., Wang, Y., Bi, C., and Zhang, X. (2019). Engineering an electroactive *Escherichia coli* for the microbial electrosynthesis of succinate from glucose and CO₂. *Microb. Cell Fact.* 18, 15. <https://doi.org/10.1186/s12934-019-1067-3>.
22. Atkinson, J.T., Su, L., Zhang, X., Bennett, G.N., Silberg, J.J., and Ajo-Franklin, C.M. (2022). Real-time bioelectronic sensing of environmental contaminants. *Nature* 611, 548–553. <https://doi.org/10.1038/S41586-022-05356-Y>.
23. Stevens, J.M., Mavridou, D.A.I., Hamer, R., Kritsiligkou, P., Goddard, A.D., and Ferguson, S.J. (2011). Cytochrome c biogenesis System I. *FEBS Journal* 278, 4170–4178. <https://doi.org/10.1111/j.1742-4658.2011.08376.x>.
24. Schuetz, B., Schicklberger, M., Kuermann, J., Spormann, A.M., and Gescher, J. (2009). Periplasmic electron transfer via the c-type cytochromes MtrA and FccA of *Shewanella oneidensis* MR-1. *Appl. Environ. Microbiol.* 75, 7789–7796. <https://doi.org/10.1128/AEM.01834-09>.
25. Fonseca, B.M., Paquete, C.M., Neto, S.E., Pacheco, I., Soares, C.M., and Louro, R.O. (2013). Mind the gap: cytochrome interactions reveal electron pathways across the periplasm of *Shewanella oneidensis* MR-1. *Biochem. J.* 449, 101–108. <https://doi.org/10.1042/BJ20121467>.
26. Sturm, G., Richter, K., Doetsch, A., Heide, H., Louro, R.O., and Gescher, J. (2015). A dynamic periplasmic electron transfer network enables respiratory flexibility beyond a thermodynamic regulatory regime. *ISME J.* 9, 1802–1811. <https://doi.org/10.1038/ismej.2014.264>.
27. Matias, V.R.F., al-Amoudi, A., Dubochet, J., and Beveridge, T.J. (2003). Cryo-transmission electron microscopy of frozen-hydrated sections of *Escherichia coli* and *Pseudomonas aeruginosa*. *J. Bacteriol.* 185, 6112–6118. <https://doi.org/10.1128/JB.185.20.6112-6118.2003>.
28. Mandela, E., Stubenrauch, C.J., Ryoo, D., Hwang, H., Cohen, E.J., Torres, V.L., Deo, P., Webb, C.T., Huang, C., Schittenhelm, R.B., et al. (2022). Adaptation of the periplasm to maintain spatial constraints essential for cell envelope processes and cell viability. *eLife* 11, e73516. <https://doi.org/10.7554/eLife.73516>.
29. Dohnalkova, A.C., Marshall, M.J., Arey, B.W., Williams, K.H., Buck, E.C., and Fredrickson, J.K. (2011). Imaging hydrated microbial extracellular polymers: comparative analysis by electron microscopy. *Appl. Environ. Microbiol.* 77, 1254–1262. <https://doi.org/10.1128/AEM.02001-10>.
30. Uden, G., and Bongaerts, J. (1997). Alternative respiratory pathways of *Escherichia coli*: energetics and transcriptional regulation in response to electron acceptors. *Biochim. Biophys. Acta* 1320, 217–234. [https://doi.org/10.1016/S0005-2728\(97\)00034-0](https://doi.org/10.1016/S0005-2728(97)00034-0).
31. Breuer, M., Rosso, K.M., Blumberger, J., and Butt, J.N. (2015). Multi-haem cytochromes in *Shewanella oneidensis* MR-1: structures, functions and opportunities. *J. R. Soc. Interface* 12, 20141117. <https://doi.org/10.1098/rsif.2014.1117>.
32. Su, L., Fukushima, T., and Ajo-Franklin, C.M. (2020). A hybrid cyt c maturation system enhances the bioelectrical performance of engineered *Escherichia coli* by improving the rate-limiting step. *Biosens. Bioelectron.* 165, 112312. <https://doi.org/10.1016/j.bios.2020.112312>.
33. Darwin, A.J., and Stewart, V. (1995). Nitrate and nitrite regulation of the Fnr-dependent aeg-46.5 promoter of *Escherichia coli* K-12 is mediated by competition between homologous response regulators (NarL and NarP) for a common DNA-binding site. *J. Mol. Biol.* 251, 15–29. <https://doi.org/10.1006/jmbi.1995.0412>.
34. Jin, M., Zhang, Q., Sun, Y., and Gao, H. (2016). NapB in excess inhibits growth of *Shewanella oneidensis* by dissipating electrons of the quinol pool. *Sci. Rep.* 6, 37456. <https://doi.org/10.1038/srep37456>.
35. Adam, F.I., Bounds, P.L., Kissner, R., and Koppenol, W.H. (2015). Redox properties and activity of iron–citrate complexes: evidence for redox cycling. *Chem. Res. Toxicol.* 28, 604–614. <https://doi.org/10.1021/tx500377b>.
36. Nellaippan, S., and Kumar, A.S. (2017). Reductive cleavage of methyl orange under formation of a redox-active hydroquinone/polyaniline nanocomposite on an electrode modified with MWCNTs, and its application to flow injection analysis of ascorbic acid at low potential and neutral pH value. *Microchim. Acta* 184, 3255–3264. <https://doi.org/10.1007/s00604-017-2339-4>.
37. Hartshorne, R.S., Reardon, C.L., Ross, D., Nuester, J., Clarke, T.A., Gates, A.J., Mills, P.C., Fredrickson, J.K., Zachara, J.M., Shi, L., et al. (2009). Characterization of an electron conduit between bacteria and the extracellular environment. *Proc. Natl. Acad. Sci. USA* 106, 22169–22174. <https://doi.org/10.1073/pnas.0900086106>.
38. Firer-Sherwood, M., Pulcu, G.S., and Elliott, S.J. (2008). Electrochemical interrogations of the Mtr cytochromes from *Shewanella*: opening a potential window. *J. Biol. Inorg. Chem.* 13, 849–854. <https://doi.org/10.1007/s00775-008-0398-z>.
39. Barrozo, A., El-Naggar, M.Y., and Krylov, A.I. (2018). Distinct electron conductance regimes in bacterial decaheme cytochromes. *Angew. Chem. Int. Ed. Engl.* 57, 6805–6809. <https://doi.org/10.1002/anie.201800294>.
40. Cai, P.J., Xiao, X., He, Y.R., Li, W.W., Chu, J., Wu, C., He, M.X., Zhang, Z., Sheng, G.P., Lam, M.H.-W., et al. (2012). Anaerobic biodecolorization mechanism of methyl orange by *Shewanella oneidensis* MR-1. *Appl. Microbiol. Biotechnol.* 93, 1769–1776. <https://doi.org/10.1007/s00253-011-3508-8>.
41. Xiao, X., Liu, Q.Y., Li, T.T., Zhang, F., Li, W.W., Zhou, X.T., Xu, M.Y., Li, Q., and Yu, H.Q. (2017). A high-throughput dye-reducing photometric assay for evaluating microbial exoelectrogenic ability. *Bioresour. Technol.* 241, 743–749. <https://doi.org/10.1016/j.biortech.2017.06.013>.
42. Stolz, A. (2001). Basic and applied aspects in the microbial degradation of azo dyes. *Appl. Microbiol. Biotechnol.* 56, 69–80. <https://doi.org/10.1007/s002530100686>.
43. Yue, W.W., Grizot, S., and Buchanan, S.K. (2003). Structural evidence for iron-free citrate and ferric citrate binding to the TonB-dependent outer membrane transporter FecA. *J. Mol. Biol.* 332, 353–368. [https://doi.org/10.1016/S0022-2836\(03\)00855-6](https://doi.org/10.1016/S0022-2836(03)00855-6).
44. Stookey, L.L. (1970). Ferrozine—a new spectrophotometric reagent for iron. *Anal. Chem.* 42, 779–781. <https://doi.org/10.1021/ac60289a016>.
45. Rountree, E.S., McCarthy, B.D., Eisenhart, T.T., and Dempsey, J.L. (2014). Evaluation of homogeneous electrocatalysts by cyclic voltammetry. *Inorg. Chem.* 53, 9983–10002. <https://doi.org/10.1021/ic500658x>.
46. Ihssen, J., Reiss, R., Luchsinger, R., Thöny-Meyer, L., and Richter, M. (2015). Biochemical properties and yields of diverse bacterial laccase-like multicopper oxidases expressed in *Escherichia coli*. *Sci. Rep.* 5, 10465. <https://doi.org/10.1038/srep10465>.
47. Brown, M.E., Mukhopadhyay, A., and Keasling, J.D. (2016). Engineering bacteria to catabolize the carbonaceous component of Sarin: teaching *E. coli* to eat isopropanol. *ACS Synth. Biol.* 5, 1485–1496. <https://doi.org/10.1021/acssynbio.6b00115>.
48. Yang, F., Hanna, M.A., and Sun, R. (2012). Value-added uses for crude glycerol—a byproduct of biodiesel production. *Biotechnol. Biofuels* 5, 13. <https://doi.org/10.1186/1754-6834-5-13>.
49. Venkateswaran, K., Moser, D.P., Dollhopf, M.E., Lies, D.P., Saffarini, D.A., MacGregor, B.J., Ringelberg, D.B., White, D.C., Nishijima, M., Sano, H., et al. (1999). Polyphasic taxonomy of the genus *Shewanella* and description of *Shewanella oneidensis* sp. nov. *Int. J. Syst. Bacteriol.* 49, 705–724. <https://doi.org/10.1099/00207713-49-2-705>.

50. Rodionov, D.A., Yang, C., Li, X., Rodionova, I.A., Wang, Y., Obratsova, A.Y., Zagnitko, O.P., Overbeek, R., Romine, M.F., Reed, S., et al. (2010). Genomic encyclopedia of sugar utilization pathways in the *Shewanella* genus. *BMC Genomics* *11*, 494. <https://doi.org/10.1186/1471-2164-11-494>.
51. Gibson, D.G., Young, L., Chuang, R.Y., Venter, J.C., Hutchison, C.A., and Smith, H.O. (2009). Enzymatic assembly of DNA molecules up to several hundred kilobases. *Nat. Methods* *6*, 343–345. <https://doi.org/10.1038/nmeth.1318>.
52. Arslan, E., Schulz, H., Zufferey, R., Künzler, P., and Thöny-Meyer, L. (1998). Overproduction of the *Bradyrhizobium japonicum* c-type cytochrome subunits of the *cbb3* oxidase in *Escherichia coli*. *Biochem. Biophys. Res. Commun.* *251*, 744–747. <https://doi.org/10.1006/bbrc.1998.9549>.
53. Malherbe, G., Humphreys, D.P., and Davé, E. (2019). A robust fractionation method for protein subcellular localization studies in *Escherichia coli*. *BioTechniques* *66*, 171–178. <https://doi.org/10.2144/btn-2018-0135>.
54. Baruch, M., Tejedor-Sanz, S., Su, L., and Ajo-Franklin, C.M. (2021). Electronic control of redox reactions inside *Escherichia coli* using a genetic module. *PLoS One* *16*, e0258380. <https://doi.org/10.1371/journal.pone.0258380>.

Joule, Volume 7

Supplemental information

**Extracellular electron transfer pathways to enhance
the electroactivity of modified *Escherichia coli***

Mohammed Mouhib, Melania Reggente, Lin Li, Nils Schuergers, and Ardemis A. Boghossian

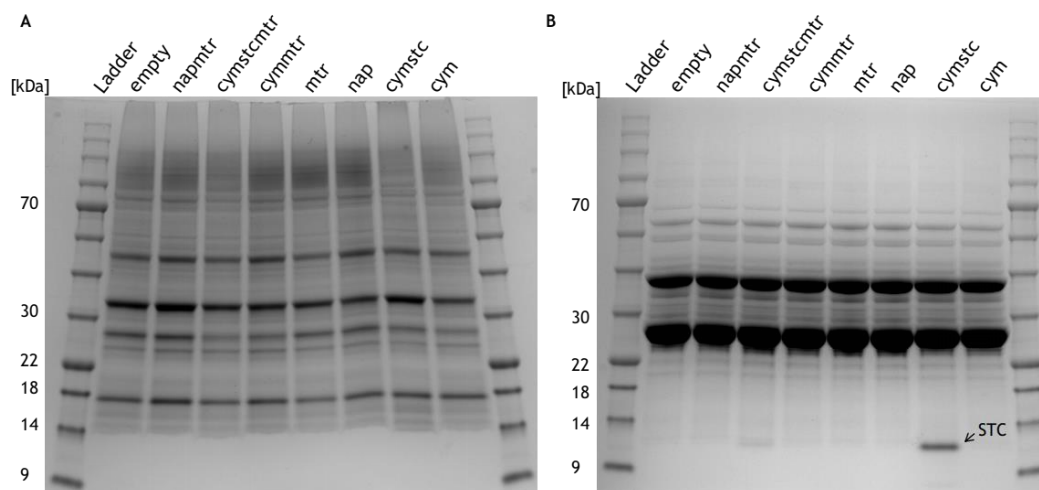


Figure S1. Coomassie brilliant blue G250 staining of SDS-PAGE gels. (A) Membrane and (B) periplasmic fractions stained after the enhanced chemiluminescence staining of the cytochromes (see Figure 1d-e in the main text).

Table S1. Overview of bacterial strains, plasmids and primers used in this study.

Strains, plasmids and primers	Characteristics	Source
Strains		
<i>E. coli</i> DH5α		
<i>E. coli</i> C43 (DE3)		
<i>S. oneidensis</i> MR-1		
Plasmids		
pEC86	CcmABCDEFGH expression, chloramphenicol resistance, tet promoter	[1]
pSB1ET2	empty backbone for cytochrome expression, kanamycin resistance, T7 promoter	[2]
pMO1	NapBC expression, kanamycin resistance, T7 promoter	This study
pMO1.1	NapBC and MtrCAB expression, kanamycin resistance, T7 promoter	This study
I5023	MtrCAB expression, kanamycin resistance, T7 promoter	[2]
pMO2	CymA and STC (<i>cctA</i> gene) expression, kanamycin resistance, T7 promoter	This study
pMO2.1	CymA, STC and MtrCAB expression, kanamycin resistance, T7 promoter	This study
I5049	CymA and MtrCAB expression, kanamycin resistance, T7 promoter	[3]
pMO2.2	CymA expression, kanamycin resistance, T7 promoter	This study
Primers		
1	5'- 3' gttttaacagggttattgcgaattctattccagcatccactaagt	
2	5'- 3' ctgcagcgccgctactagttagattagagttgttaactcatgctca	
3	5'- 3' agaagtaattgccgctgcaaGaattctattccagcatccactaagtc	
4	5'- 3' ctgcagcgccgctactagttag	
5	5'- 3' gttacaaactctaatactagaactagtagcgccgctgcag	
6	5'- 3' ggatgctggaaatagaattcgcaataaccctgttaaaaacctggc	
7	5'- 3' gttacaaactctaatactagaactagtagcgccgctgcag	
8	5'- 3' ggatgctggaaatagaattCttgcagcggaattactcttc	

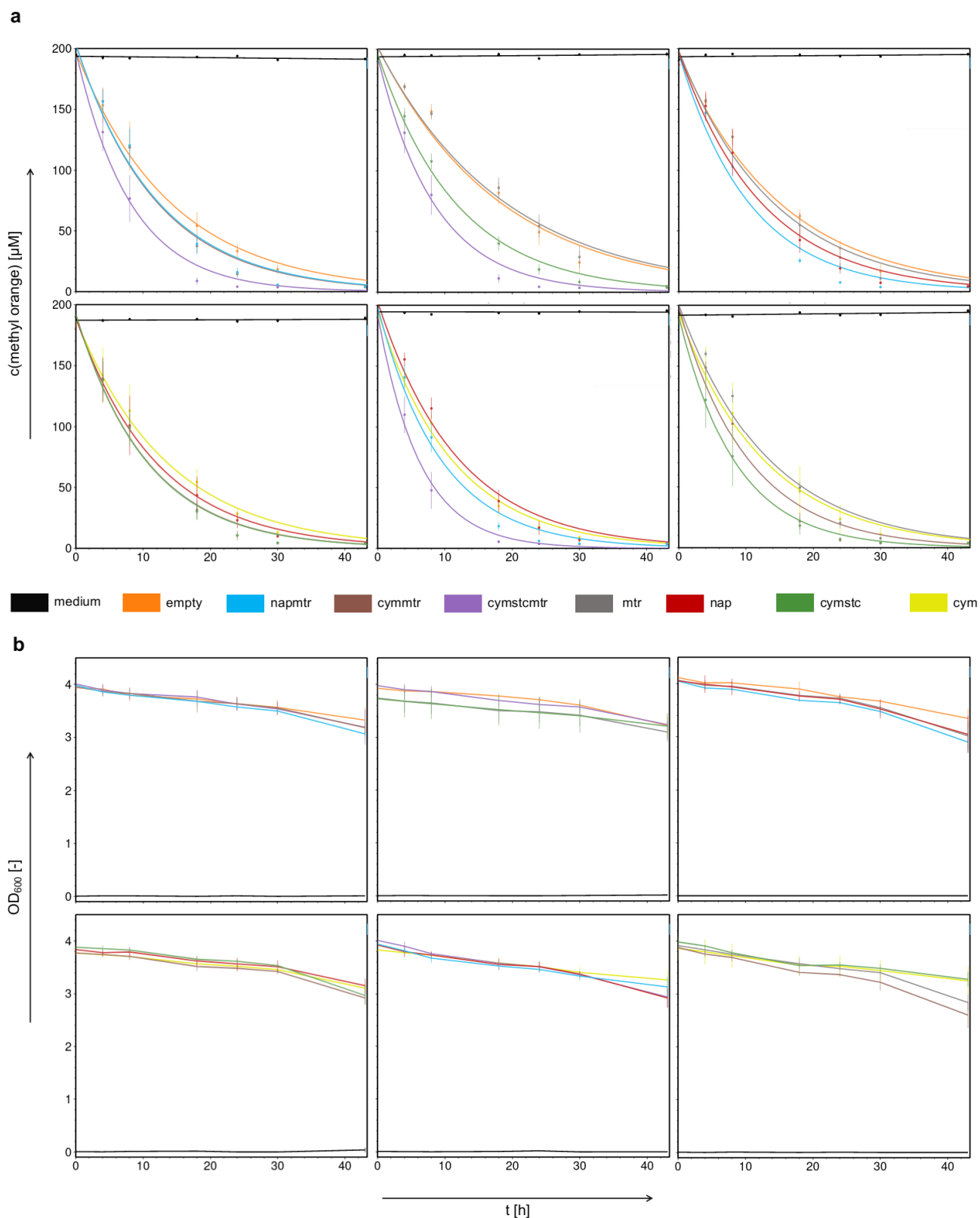


Figure S2. Methyl orange reduction assay. Individual replicate plots of (a) methyl orange concentration and (b) OD_{600} in assay tubes over 2 days. Experiments were carried out with four biological replicates per strain, and all strains were used in three separate experiments for a total of 12 replicates. Dots and bars represent average values and one standard deviation over four samples.

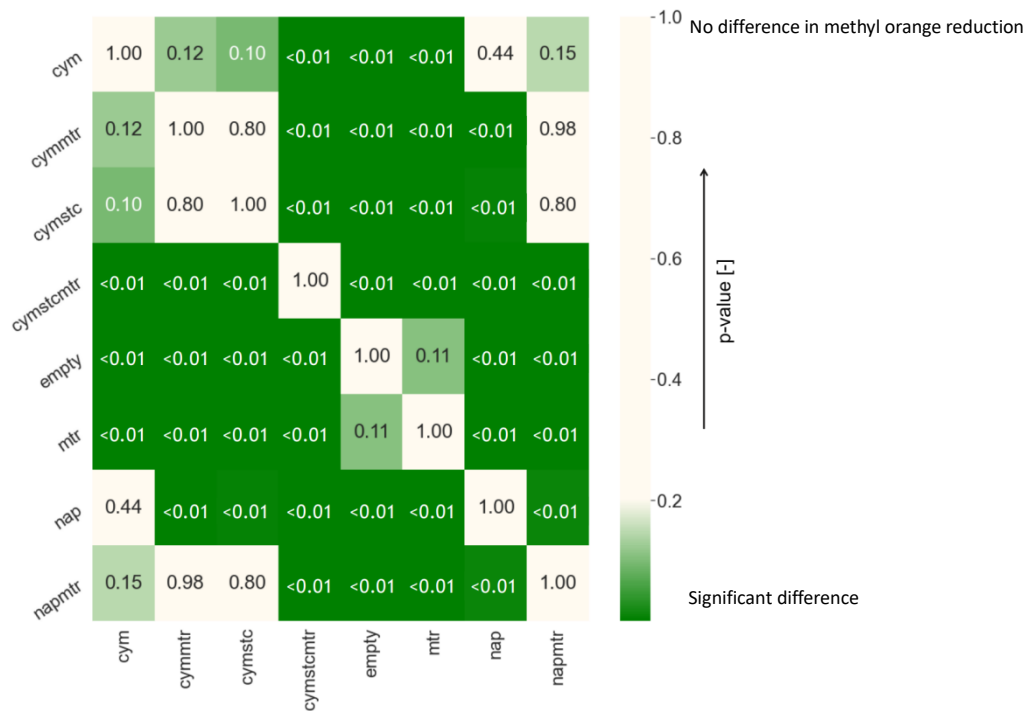


Figure S3. Comparative analysis of methyl orange reduction rates for different strains. P values obtained from two tailed two sample T-tests without assuming equal population variance (Welch's T-test) plotted against each strain pair. Smaller p-values (darker green) correspond to more significant differences between the strains. The analysis was performed on data shown in Figure 2b of the main text.

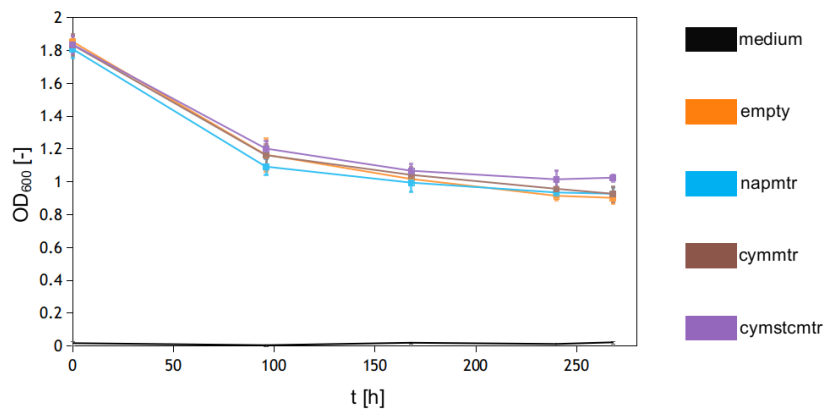


Figure S4. Measurements of the OD₆₀₀ over the course of 11 days during ferric citrate reduction assays. Data is shown as the mean of four biological replicates, with error bars indicating one standard deviation.

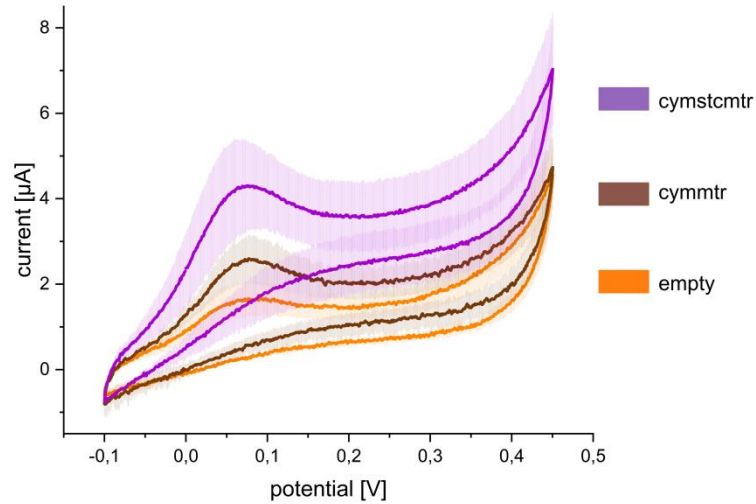


Figure S5. Cyclic voltammetry (CV) of different strains after chronoamperometry. CV measurements were performed at a scan rate of 2 mV/s, immediately after chronoamperometry (see main text, Figure 3). Data is shown for the last out of three cycles, with solid lines indicating the mean current and shaded areas indicating one standard deviation between three biological replicates per strain.

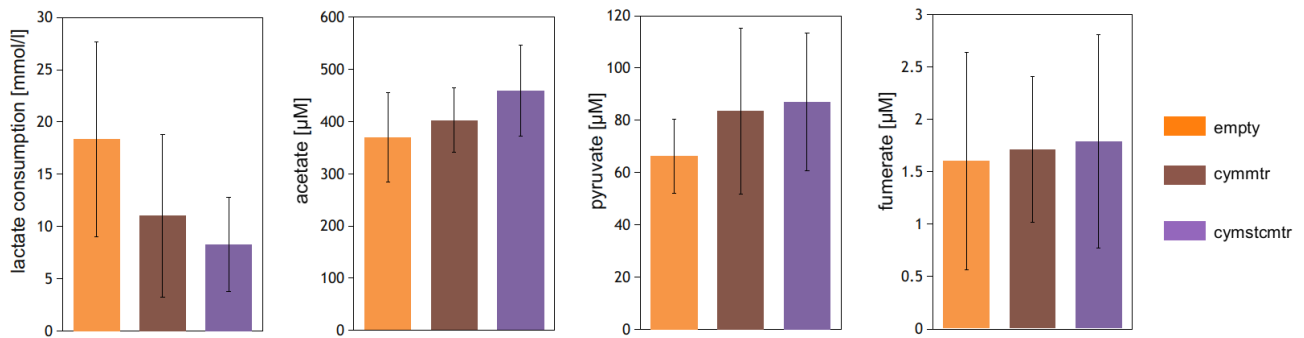


Figure S6. Lactate consumption and concentration of different fermentation products after chronoamperometric measurements in lactate-fueled electrochemical cells.

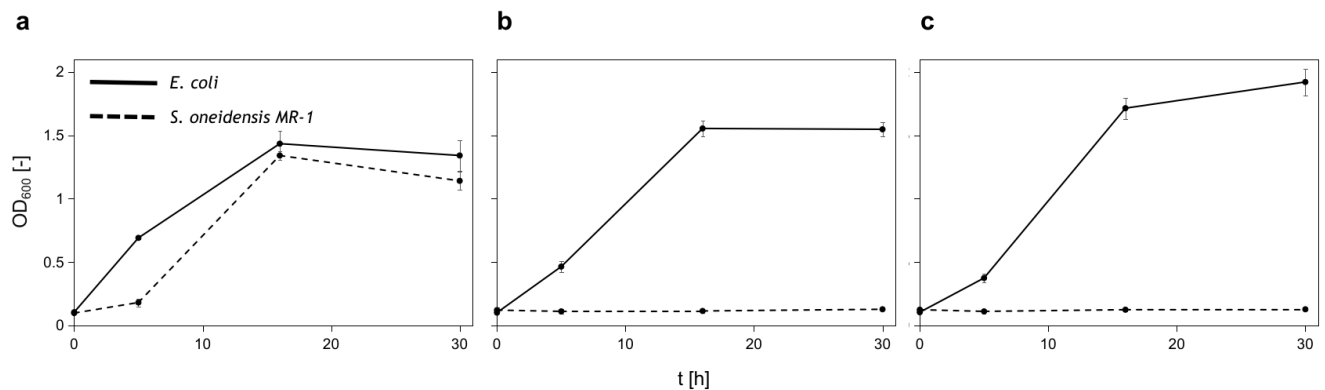


Figure S7. M9-medium supplemented with lactate (a), glycerol (b) and xylose (c) as growth substrates for *E. coli* and *S. oneidensis* MR-1. Bacterial growth over time was determined using OD₆₀₀ measurements from aerobic culture flasks kept under constant shaking at 30°C (*S. oneidensis* MR-1) and 37°C (*E. coli* C43(DE3)). Data is shown as the mean of three biological replicates, with error bars indicating one standard deviation.

Supplemental references

- [1] Arslan, E., Schulz, H., Zufferey, R., Künzler, P., and Thöny-Meyer, L. (1998). Overproduction of the *Bradyrhizobium japonicum* c-Type Cytochrome Subunits of the *cbb3* Oxidase in *Escherichia coli*. *Biochem Biophys Res Commun* 251, 744–747. 10.1006/bbrc.1998.9549.
- [2] Jensen, H.M., Albers, A.E., Malley, K.R., Londer, Y.Y., Cohen, B.E., Helms, B.A., Weigele, P., Groves, J.T., and Ajo-Franklin, C.M. (2010). Engineering of a synthetic electron conduit in living cells. *Proc Natl Acad Sci U S A* 107, 19213–19218. 10.1073/pnas.1009645107.
- [3] Jensen, H.M., TerAvest, M.A., Kokish, M.G., and Ajo-Franklin, C.M. (2016). CymA and Exogenous Flavins Improve Extracellular Electron Transfer and Couple It to Cell Growth in Mtr-Expressing *Escherichia coli*. *ACS Synth Biol* 5, 679–688. 10.1021/acssynbio.5b00279.